

Equatorial light bending around Kerr-Newman black holes

You-Wei Hsiao,^{*} Da-Shin Lee,[†] and Chi-Yong Lin[‡]

Department of Physics, National Dong Hwa University,

Hualien, Taiwan, Republic of China

(Dated: April 15, 2020)

Abstract

We study the deflection angle of a light ray as it traverses on the equatorial plane of a charged spinning black hole. We provide detailed analysis of the light ray's trajectory, and derive the closed-form expression of the deflection angle due to the black hole in terms of elliptic integrals. In particular, the geodesic equation of the light ray along the radial direction can be used to define an appropriate "effective potential". The nonzero charge of the black hole shows stronger repulsive effects to prevent light rays from falling into the black hole as compared with the Kerr case. As a result, the radius of the innermost circular motion of light rays with the critical impact parameter decreases as charge Q of the black hole increases for both direct and retrograde motions. Additionally, the deflection angle decreases when Q increases with the fixed impact parameter. These results will have a direct consequence on constructing the apparent shape of a charged rotating black hole.

PACS numbers: 04.70.-s, 04.70.Bw, 04.80.Cc

^{*}Electronic address: hsiao.phys@gapp.nthu.edu.tw

[†]Electronic address: dslee@gms.ndhu.edu.tw

[‡]Electronic address: lyong@gms.ndhu.edu.tw

I. INTRODUCTION

General relativity provides a unified description of gravity as a geometric property of spacetime [1, 2]. In particular, the presence of matter and radiation with energy and momentum can curve spacetime, and the light ray's trajectory will be deflected as a chief effect [3]. One of the very important consequences of general relativity is the bending of a light ray in the presence of a gravitational field. In the light of the first image of the black hole captured by the Event Horizon Telescope [4–6], these rays will yield the apparent shadow of the black hole for an observer in the asymptotic region, and the understanding of the shadows becomes very important for measuring the properties of astrophysical black holes.

Light deflection in weak gravitational field of Schwarzschild black holes was known in 1919, and served as the starting point to develop gravitational lensing theory. Nevertheless, light deflection in the strong gravitational field of Schwarzschild black holes was not studied until several decades ago by Darwin [7]. It was then reexamined in [8–11], and extended to the Reissner-Nordstrom spacetime or charged black holes [12–15], and to any spherically symmetric black holes [16]. Black hole lenses were also explored numerically by [17–19]. Kerr black hole lenses were analyzed in [20–26], which, in particular, found rotating black hole apparent shapes or shadows with an optical deformation rather than being circles as in the case of nonrotating ones [27–33]. The bending angle of light rays due to Kerr black holes on the equatorial plane was studied analytically in [34–37] using the null geodesic equations. The deflections produced in the presence of a rotating black hole explicitly depend on the direction of motion of the light relative to the spin direction of the black hole. In particular, the authors of [34] derived the closed-form expression of the equatorial light deflection angle in terms of elliptic integrals. However, the strong gravitation field gives rise to the large bending of light rays near a black hole. The bending angle can be larger than 2π , showing the possibility that light rays might go around the center of the black hole several times before reaching the observer. Apart from a primary image, a theoretically infinite sequence of images, which we term relativistic images, might be formed, and are usually greatly demagnified. The closed-form expression of the light bending angle in an exact result [34] or in some sort of asymptotic approximation might be of great help to study these images [36, 37], although the observation of relativistic images is a very difficult task.

Another known asymptotically flat and stationary solution of the Einstein-Maxwell field

equations in general relativity is the Kerr-Newman metric, a generalization of the Kerr metric, which describes spacetime in the exterior of a rotating charged black hole. Apart from gravitation fields, both electric and magnetic fields exist intrinsically from the black hole. Although one might not expect that astrophysical black holes have a large residue electric charge, some accretion scenarios were proposed to investigate the possibility of the spinning charged black holes [38]. It is then still of great interest to extend the previous studies to a Kerr-Newman black hole [39–42]. The central thread of this paper is to try to achieve the exact expression of the light deflection angle by a Kerr-Newman black hole in the equatorial plane, an extension of the work in [34] for the Kerr black hole case. In Sec.II, we focus on circular trajectories of light rays arriving from and returning to spatial infinity. Their null geodesic equations along the radial direction on the equatorial plane of the black hole can be analogously realized as particle motion in the effective potential. Section III explores the effects of the black hole charge on the circular trajectories via this effective potential. In particular, we solve the geodesic equations to find the radius of innermost circular trajectories and its corresponding impact parameter in terms of the black hole’s parameters. Section IV derives a closed-form expression for the equatorial light deflection angle. We have verified that, by taking the limit of $Q = 0$, our result reduces to the case of the Kerr black hole obtained by work [34]. All results will be summarized in the closing section.

II. GEODESIC EQUATIONS AND INNERMOST CIRCULAR TRAJECTORIES OF LIGHT RAYS IN KERR-NEWMAN SPACETIME

In this paper, we thoroughly study the light bending due to the Kerr-Newman black hole, in which spacetime outside a black hole with the gravitational mass M , charge Q , and angular momentum per unit mass $a = J/M$ is described by the Kerr-Newman metric as

$$\begin{aligned}
 ds^2 &= g_{\mu\nu} dx^\mu dx^\nu \\
 &= -\frac{(\Delta - a^2 \sin^2 \theta)}{\Sigma} dt^2 + \frac{a \sin^2 \theta (Q^2 - 2Mr)}{\Sigma} (dt d\phi + d\phi dt) \\
 &\quad + \frac{\Sigma}{\Delta} dr^2 + \Sigma d\theta^2 + \frac{\sin^2 \theta}{\Sigma} ((r^2 + a^2)^2 - a^2 \Delta \sin^2 \theta) d\phi^2, \tag{1}
 \end{aligned}$$

where

$$\Sigma = r^2 + a^2 \cos^2 \theta, \quad \Delta = r^2 + a^2 + Q^2 - 2Mr. \tag{2}$$

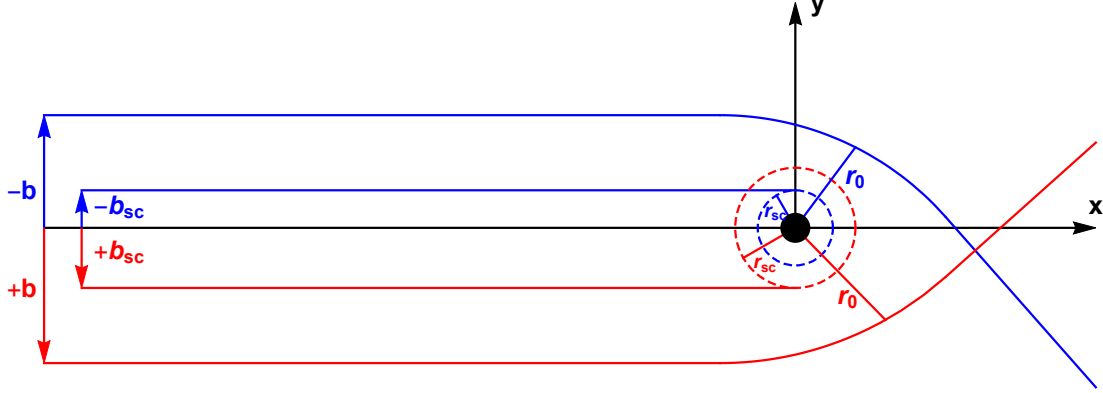


FIG. 1: Sign convention for orbits as viewed from above. The spin axis of the black hole points out of the page in this figure. The red (blue) solid line shows the direct (retrograde) orbit with the radius of closest approach r_0 . The suffix "c" is added in the case of the innermost circular motion.

The event horizon R_H can be found by solving $\Delta(r) = 0$, and is given by

$$R_H = M + \sqrt{M^2 - (Q^2 + a^2)} \quad (3)$$

with the condition $M^2 > Q^2 + a^2$. The Lagrangian of a particle is then

$$\mathcal{L} = \frac{1}{2} g_{\mu\nu} u^\mu u^\nu \quad (4)$$

with the 4-velocity $u^\mu = dx^\mu/d\lambda$ defined in terms of an affine parameter λ .

Due to the fact that the metric of the Kerr-Newman black hole is independent of t and ϕ , the associated Killing vectors are $\xi_{(t)}^\mu$ and $\xi_{(\phi)}^\mu$ given, respectively, by

$$\xi_{(t)}^\mu = \delta_t^\mu, \quad \xi_{(\phi)}^\mu = \delta_\phi^\mu. \quad (5)$$

Then, together with the 4-velocity of light rays, the conserved quantities, namely energy and azimuthal angular momentum, along a geodesic, can be constructed by the above Killing vectors

$$\varepsilon \equiv -\xi_{(t)}^\mu u_\mu = \frac{1}{\Sigma} \left[a (\ell - \varepsilon a \sin^2 \theta) + \frac{(r^2 + a^2) [\varepsilon(r^2 + a^2) - a\ell]}{\Delta} \right], \quad (6)$$

$$\ell \equiv \xi_{(\phi)}^\mu u_\mu = \frac{1}{\Sigma} \left[\frac{\ell - a\varepsilon \sin^2 \theta}{\sin^2 \theta} + \frac{a [\varepsilon(r^2 + a^2) - a\ell]}{\Delta} \right], \quad (7)$$

where ε and ℓ are the light ray's energy and azimuthal angular momentum evaluated at spatial infinity. Light rays travel along null world lines obeying the condition $u^\mu u_\mu = 0$.

Additionally, there exists a Carter constant

$$\kappa = u_\mu u_\nu K^{\mu\nu} - (\ell - a\varepsilon)^2, \quad (8)$$

where

$$\begin{aligned} K^{\mu\nu} &= \Delta k^\mu q^\nu + r^2 g^{\mu\nu}, \\ q^\mu &= \frac{1}{\Delta} [(r^2 + a^2)\delta_t^\mu + \Delta\delta_r^\mu + a\delta_\phi^\mu], \\ k^\mu &= \frac{1}{\Delta} [(r^2 + a^2)\delta_t^\mu - \Delta\delta_r^\mu + a\delta_\phi^\mu]. \end{aligned} \quad (9)$$

Using these three constants of motion together with $u_\mu u^\mu = 0$, we are able to write down the general geodesic equations for light rays in terms of ε , ℓ , and κ as

$$\Sigma \dot{t} = -a (a\varepsilon \sin^2 \theta - \ell) + \frac{(r^2 + a^2) [\varepsilon(r^2 + a^2) - a\ell]}{\Delta}, \quad (10)$$

$$\Sigma \dot{\phi} = - \left(a\varepsilon - \frac{\ell}{\sin^2 \theta} \right) + \frac{a [\varepsilon(r^2 + a^2) - a\ell]}{\Delta}, \quad (11)$$

$$\Sigma^2 \dot{r}^2 = (\varepsilon(r^2 + a^2) - a\ell)^2 - \Delta [(\ell - a\varepsilon)^2 + \kappa], \quad (12)$$

$$\Sigma^2 \dot{\theta}^2 = \kappa + \cos^2 \theta \left(a^2 \varepsilon^2 - \frac{\ell^2}{\sin^2 \theta} \right). \quad (13)$$

The overdot means the derivative with respect to the affine parameter λ . To indicate whether the light ray is traversing along the direction of frame dragging or opposite to it, we define the following impact parameter :

$$b_s = s \left| \frac{\ell}{\varepsilon} \right| \equiv s b, \quad (14)$$

where $s = \text{Sign}(\ell/\varepsilon)$ and b is the positive magnitude. The parameter $s = +1$ for $b_s > 0$ will be referred to as direct orbits; and those with $s = -1$ for $b_s < 0$ as retrograde orbits (see Fig.1 for the sign convention).

Here we restrict the light rays traveling on the equatorial plane of the black hole by choosing $\theta = \pi/2$, and $\dot{\theta} = 0$, so that $\kappa = 0$ in Eq. (13). Rewriting the equation of motion along the radial direction, (12) allows us to define the function W_{eff} from

$$\frac{1}{b^2} = \frac{\dot{r}^2}{\ell^2} + W_{\text{eff}}(r), \quad (15)$$

where

$$W_{\text{eff}}(r) = \frac{1}{r^2} \left[1 - \frac{a^2}{b^2} + \left(-\frac{2M}{r} + \frac{Q^2}{r^2} \right) \left(1 - \frac{a}{b_s} \right)^2 \right]. \quad (16)$$

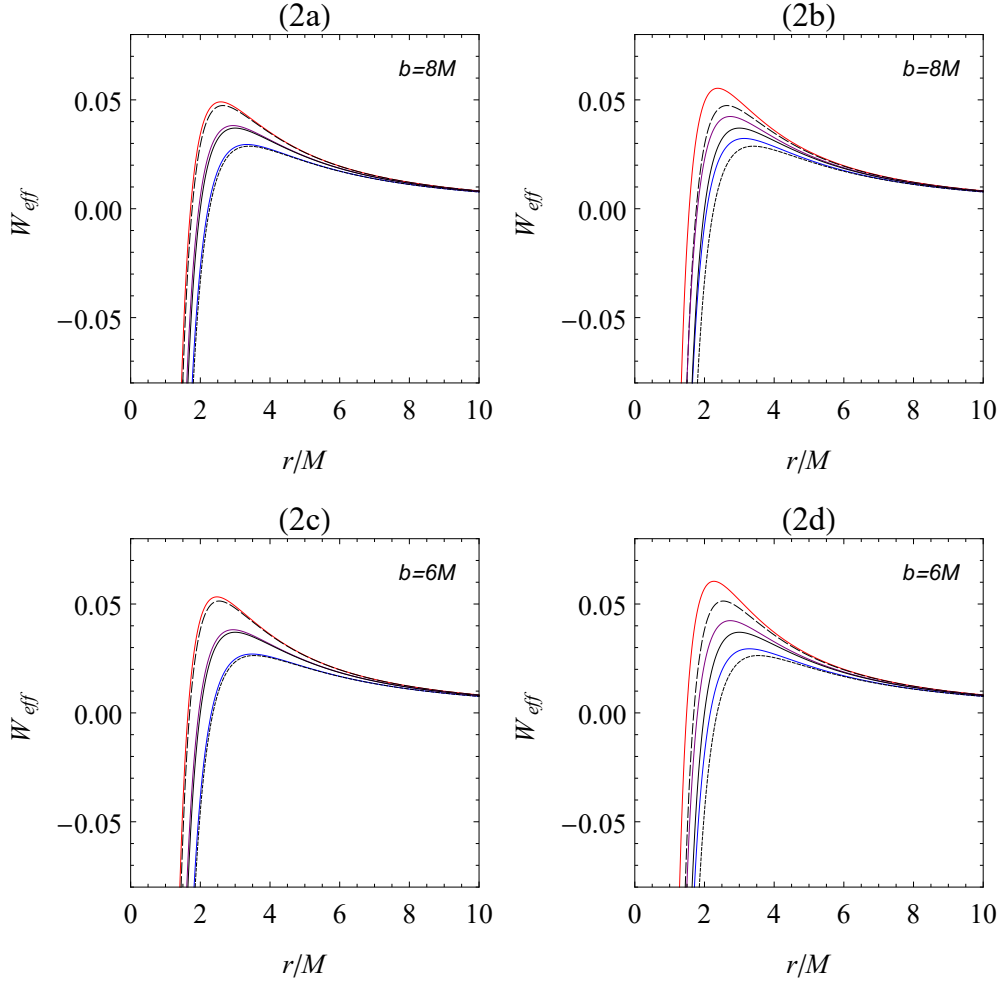


FIG. 2: The the “effective potential” W_{eff} as a function of r/M for four sets of parameters. (a) $a/M = 0.5$, $Q/M = 0.3$, and $b = 8M$; (b) $a/M = 0.5$, $Q/M = 0.6$, and $b = 8M$; (c) $a/M = 0.5$, $Q/M = 0.3$, and $b = 6M$; (d) $a/M = 0.5$, $Q/M = 0.6$, and $b = 6M$. The plot convention used henceforth: Kerr-Newman direct (red), Kerr-Newman retrograde (blue), Kerr direct (dashed with $Q = 0$), Kerr retrograde (dotted with $Q = 0$), Reissner-Nordstrom (purple with $a = 0$), and Schwarzschild (black with $Q = 0, a = 0$). The nonzero charge of the black hole gives more repulsive effects to the light rays as seen from the effective potential than the corresponding black hole with zero Q .

The above equation is analogous to that of particle motion in the effective potential $W_{\text{eff}}(r)$ shown in Fig.2 with the kinetic energy \dot{r}^2/ℓ^2 and constant total energy $1/b^2$ [2, 40].

In the limits of $Q = 0$ and $Q = 0, a = 0$, the effective potential W_{eff} reduces to the ones for the Kerr and Schwarzschild black holes respectively [2]. In the case of the Kerr-Newman

black hole, the nonzero charge of the black hole seems to give repulsive effects to the light rays as seen from its contributions to the centrifugal potential of the $1/r^2$ term. These repulsive forces in turn affect light rays so as to prevent them from collapsing into the event horizon, and thus as will be seen later, shift the innermost circular trajectories of the light rays toward the black hole. Also, the presence of the black hole's charge is found to decrease the deflection angle due to this additional repulsive effect on the light rays, as compared with Kerr's case for the same impact parameter b .

To see it, let us consider a light ray that starts in the asymptotic region to approach the black hole, and then turn back to the asymptotic region to reach the observer. Such light rays have a turning point, the radius of closest approach to a black hole r_0 , which crucially depends on the impact parameter b , determined by

$$\left. \frac{\dot{r}^2}{\ell^2} \right|_{r=r_0} = \frac{1}{b^2} - W_{\text{eff}}(r_0) = 0. \quad (17)$$

Equation (17) leads to a quartic equation in r_0

$$r_0^4 - b^2 \left(1 - \frac{a^2}{b^2}\right) r_0^2 + 2Mb^2 \left(1 - \frac{a}{b_s}\right)^2 r_0 - Q^2 b^2 \left(1 - \frac{a}{b_s}\right)^2 = 0. \quad (18)$$

We express the solutions in terms of trigonometric functions, where one of the three roots of (18) gives the analytical result of r_0 as

$$r_0(b_s) = \frac{b}{\sqrt{6}} \sqrt{1 - \omega_s^2} \left\{ \sqrt{1 + \sqrt{1 - \Omega_s} \cos\left(\frac{2\Theta}{3}\right)} + \sqrt{2 - \sqrt{1 - \Omega_s} \cos\left(\frac{2\Theta}{3}\right) - \frac{3\sqrt{6}M(1 - \omega_s)^2}{b(1 - \omega_s^2)^{\frac{3}{2}} \sqrt{1 + \sqrt{1 - \Omega_s} \cos\left(\frac{2\Theta}{3}\right)}}} \right\} \quad (19)$$

with ω_s , Ω_s and Θ , depending explicitly on the black hole's parameters, as well as the impact parameter b_s , defined as

$$\begin{aligned} \omega_s &= \frac{a}{b_s}, \\ \Omega_s &= \frac{12Q^2}{b^2(1 + \omega_s)^2}, \\ \Theta &= \arccos \left(\frac{3\sqrt{3}M(1 - \omega_s)^2}{b(1 - \omega_s^2)^{\frac{3}{2}}(1 - \Omega_s)^{\frac{3}{4}}} \sqrt{1 - \frac{b^2(1 + \omega_s)^3}{54M^2(1 - \omega_s)} \left[1 + 3\Omega_s - (1 - \Omega_s)^{\frac{3}{2}}\right]} \right). \end{aligned} \quad (20)$$

In the case of the Kerr black hole with $Q = 0$, we have

$$\begin{aligned}\Omega_s &= 0, \\ \Theta &= \arccos\left(\frac{3\sqrt{3}M(1-\omega_s)^2}{b(1-\omega_s^2)^{\frac{3}{2}}}\right).\end{aligned}$$

Equation (19) reduces to $r_0(b)$ in [34] as

$$\begin{aligned}r_0(b_s) &= \frac{b}{\sqrt{6}}\sqrt{1-\omega_s^2}\left\{\sqrt{1+\cos\left(\frac{2\Theta}{3}\right)}+\sqrt{2-\cos\left(\frac{2\Theta}{3}\right)-\frac{3\sqrt{6}M(1-\omega_s)^2}{b(1-\omega_s^2)^{\frac{3}{2}}\sqrt{1+\cos\left(\frac{2\Theta}{3}\right)}}}\right\} \\ &= \frac{2b}{\sqrt{3}}\sqrt{1-\frac{a^2}{b^2}}\cos\left[\frac{1}{3}\arccos\left(\frac{-3\sqrt{3}M\left(1-\frac{a}{b_s}\right)^2}{b\left(1-\frac{a^2}{b^2}\right)^{\frac{3}{2}}}\right)\right].\end{aligned}$$

The distance of closest approach r_0 for the light ray to travel around Kerr-Newman black holes, given in Eq.(19), certainly generalizes that of the Kerr or the Schwarzschild black holes depicted in Fig.3.

It is anticipated that for both direct and retrograde motions, the repulsive effect from the charge of black holes pushes the distance of closest approach r_0 being away from the black hole for a fixed impact parameter b , which can be compared with the Kerr case with the same impact parameter b .

III. CRITICAL IMPACT PARAMETERS AND INNERMOST CIRCULAR ORBITS

Again, consider the light rays coming in from spatial infinity with the impact parameter b . The plots in Fig. 2 show the shape of the effective potential $W_{\text{eff}}(r)$ that vanishes at large r and has one maximum. The behavior of the light ray trajectories depends on whether $1/b^2$ is greater or less than the maximum height of $W_{\text{eff}}(r)$. The innermost trajectories of light rays have a direct consequence on the apparent shape of the black hole with the smallest radius r_c when the turning point r_0 is located at the maximum of $W_{\text{eff}}(r)$ for a particular choice of b_c obeying

$$\left.\frac{dW_{\text{eff}}(r)}{dr}\right|_{r=r_{sc}} = 0 \quad (21)$$

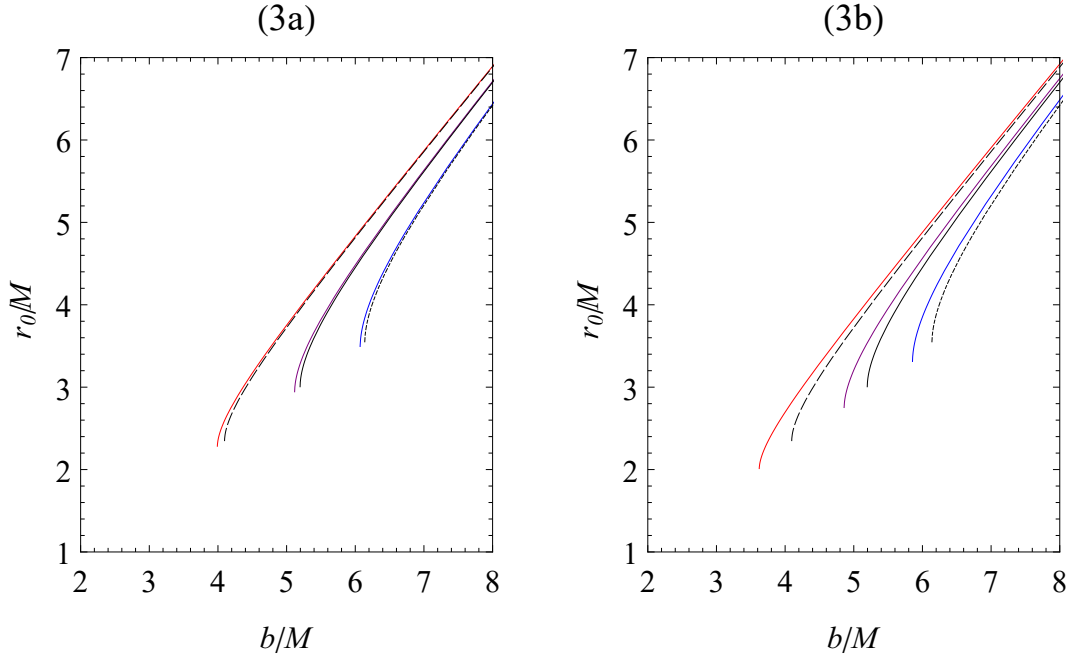


FIG. 3: The distance of closest approach r_0/M as a function of the impact parameter b/M for (a) $a/M = 0.5$ and $Q/M = 0.3$; (b) $a/M = 0.5$ and $Q/M = 0.6$. The plots show the results for the Schwarzschild, Reissner-Nordström, Kerr and Kerr-Newman black holes for comparison. The additional repulsive effects from the charge of the black hole pushes the distance of closest approach r_0 of light rays being away from the black hole for a fixed impact parameter b .

with the value

$$r_{sc} = \frac{3M}{2} \left(\frac{1 - \frac{a}{b_{sc}}}{1 + \frac{a}{b_{sc}}} \right) \left[1 + \sqrt{1 - \frac{8Q^2 \left(1 + \frac{a}{b_{sc}}\right)}{9M^2 \left(1 - \frac{a}{b_{sc}}\right)}} \right], \quad (22)$$

which is a circular motion forming a photon sphere. However, these circular trajectories are unstable because any small change in b results in the trajectory moving away from the maximum. The radius of the circular photon orbit r_{sc} above is consistent with the finding in [3], and the known result of r_{sc} in the limit $Q = 0$ given in [34]. We then substitute (22) into (18) for obtaining the corresponding critical impact parameter b_{sc} .

Substituting (22) into (18), it is more convenient to express the equations in terms of y_+

and y_- , respectively [34],

$$y_+ = b_{+c} + a, \quad (23)$$

$$y_- = -(b_{-c} + a), \quad (24)$$

which obey the quartic equations

$$(Q^2 - M^2)y_+^4 + 2M^2ay_+^3 + (27M^4 - 36M^2Q^2 + 8Q^4)y_+^2 - (108M^4a - 72M^2Q^2a)y_+ + (108M^4a^2 + 16Q^6) = 0, \quad (25)$$

$$(Q^2 - M^2)y_-^4 - 2M^2ay_-^3 + (27M^4 - 36M^2Q^2 + 8Q^4)y_-^2 + (108M^4a - 72M^2Q^2a)y_- + (108M^4a^2 + 16Q^6) = 0. \quad (26)$$

The solutions of the critical value b_{sc} in a Kerr-Newman black hole are found analytically to be

$$b_{sc} = -a + \frac{M^2a}{2(M^2 - Q^2)} + \frac{s}{2\sqrt{3}(M^2 - Q^2)} \left[\sqrt{V + (M^2 - Q^2) \left(U + \frac{P}{U} \right)} + \sqrt{2V - (M^2 - Q^2) \left(U + \frac{P}{U} \right) - \frac{s6\sqrt{3}M^2a [(M^2 - Q^2)(9M^2 - 8Q^2)^2 - M^4a^2]}{\sqrt{V + (M^2 - Q^2) \left(U + \frac{P}{U} \right)}}} \right] \quad (27)$$

where

$$\begin{aligned} P &= (3M^2 - 4Q^2) [9(3M^2 - 4Q^2)^3 + 8Q^2(9M^2 - 8Q^2)^2 - 216M^4a^2], \\ U &= \left\{ - [3(3M^2 - 2Q^2)^2 - 4Q^4] [9M^2(9M^2 - 8Q^2)^3 - 8 [3(3M^2 - 2Q^2)^2 - 4Q^4]^2] \right. \\ &\quad + 108M^4a^2 [9(3M^2 - 4Q^2)^3 + 4Q^2(9M^2 - 8Q^2)^2 - 54M^4a^2] \\ &\quad \left. + 24\sqrt{3}M^2 \sqrt{(M^2 - a^2 - Q^2) [Q^2(9M^2 - 8Q^2)^2 - 27M^4a^2]^3} \right\}^{\frac{1}{3}}, \\ V &= 3M^4a^2 + (M^2 - Q^2) [6(3M^2 - 2Q^2)^2 - 8Q^4]. \end{aligned} \quad (28)$$

Although one can numerically check the consistency between the expression of (27) in the limit of $Q = 0$ and that of the Kerr case given by [34]

$$b_{sc} \rightarrow -a + s6M \cos \left[\frac{1}{3} \cos^{-1} \left(\frac{-sa}{M} \right) \right], \quad (29)$$

direct simplification to recover (29), by setting $Q = 0$ in (27), is not so trivial to achieve. An alternative consistency check is to consider that the above two quartic equations (25)

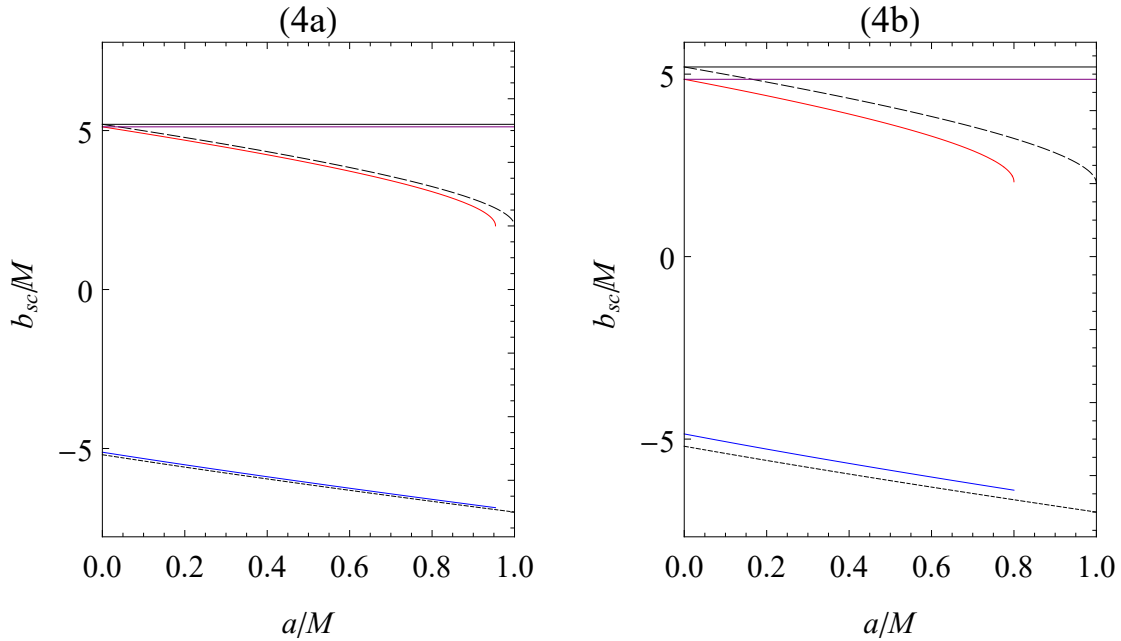


FIG. 4: The critical impact parameter b_{sc}/M as a function of the spin parameter a/M for (a) $Q/M = 0.3$, (b) $Q/M = 0.6$. The plots show the Schwarzschild, Reissner-Nordstrom, Kerr and Kerr-Newman black holes for comparison. The circular orbits exist for a charged black hole with the smaller impact parameter $|b_{sc}|$ as compared with the corresponding black hole with $Q = 0$ for the same a .

and (26) in the limit of Kerr case, $Q = 0$ lead to

$$-M^2(y_+ - 2a)(y_+^3 - 27M^2y_+ + 54M^2a) = 0, \quad (30)$$

$$-M^2(y_- + 2a)(y_-^3 - 27M^2y_- - 54M^2a) = 0. \quad (31)$$

Their solutions certainly give (29) using (23) and (24). Then, the radius of innermost circular trajectories r_{sc} with the impact parameter b_{sc} can be obtained through (22), which will be a tedious function of the black hole's parameters.

According to [42], in fact, the equation to determine the radius of innermost circular motions r_c in terms of the black hole's parameters can be derived directly. Let us consider a particle with mass m moving around the Kerr-Newman black hole. There exists the circular motion of the particle with the radius r when the energy E and azimuthal angular

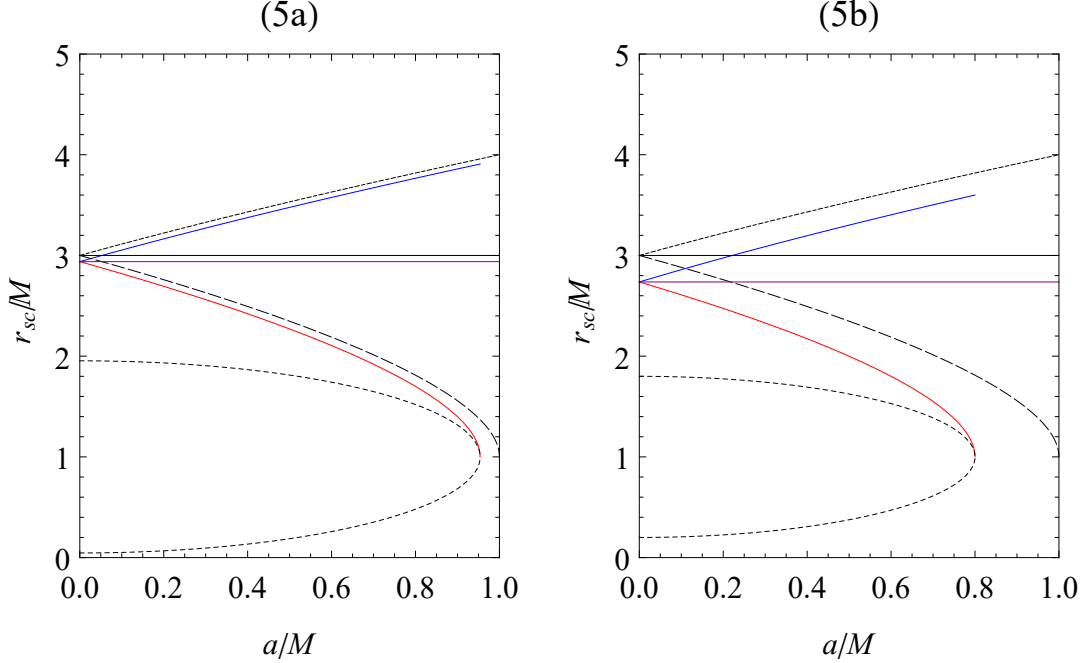


FIG. 5: The critical radius r_{sc}/M plotted as a function of the spin parameter for (a) $Q/M = 0.3$, (b) $Q/M = 0.6$. The cases of r_{sc} of the Schwarzschild, Reissner-Nordstrom, Kerr and Kerr-Newman black holes are drawn for comparison. Additionally, the Kerr-Newman outer(inner) horizon radii are shown in red(orange) dashed line for reference. The circular orbits exist for a charged black hole with a smaller value of the radius r_{sc} as compared with the corresponding black hole with $Q = 0$ for a fixed a .

momentum L satisfy [39, 43]

$$\frac{E}{m} = \frac{a\sqrt{Mr - Q^2} + (Q^2 + r^2 - 2Mr)}{r\sqrt{2Q^2 + r^2 - 3Mr + 2a(Mr - Q^2)^{1/2}}}, \quad (32)$$

$$\frac{L}{m} = \frac{a(Q^2 - 2Mr) + (a^2 + r^2)\sqrt{Mr - Q^2}}{r\sqrt{2Q^2 + r^2 - 3Mr + 2a(Mr - Q^2)^{1/2}}}. \quad (33)$$

Apparently, the radius of the circular motion cannot be arbitrarily small. In particular, in the case of massless limit ($m \rightarrow 0$), the conditions of having finite values of E and L require the radius of the circular photon orbit obeying

$$2Q^2 + r_c^2 - 3Mr_c + 2a(Mr_c - Q^2)^{1/2} = 0. \quad (34)$$

In the limit of $Q = 0$, we have one of the roots given by

$$r_{sc} = 2M \left\{ 1 + \cos \left[\frac{2}{3} \cos^{-1} \left(\frac{-sa}{M} \right) \right] \right\} \quad (35)$$

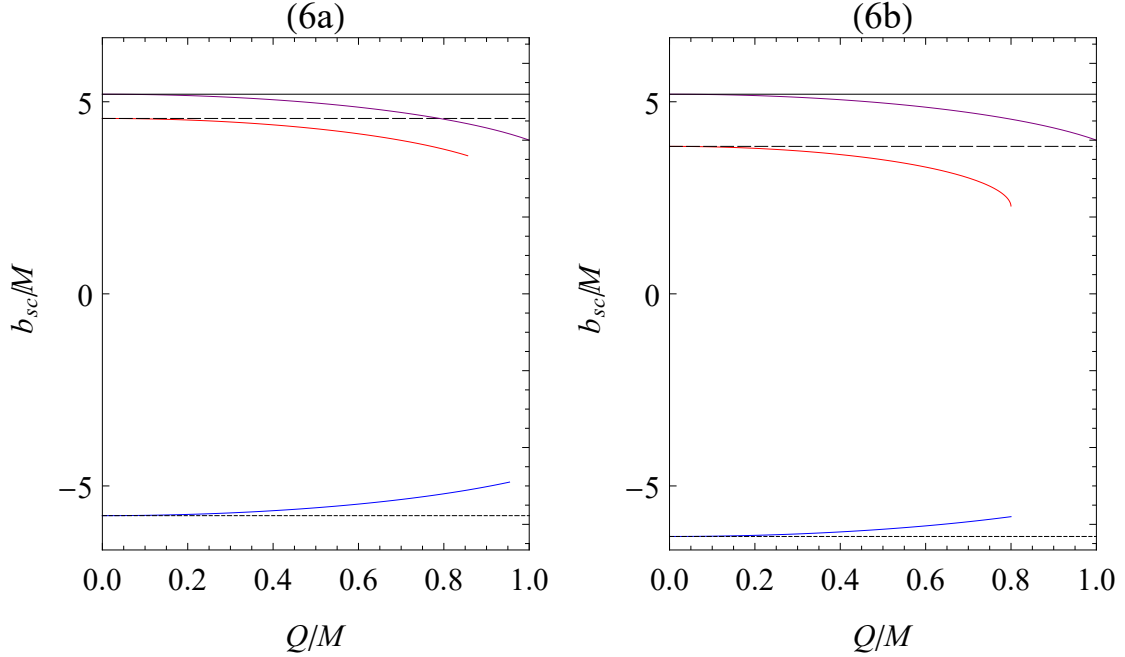


FIG. 6: The critical impact parameter b_{sc}/M as a function of charge Q/M for (a) $a/M = 0.3$, (b) $a/M = 0.6$. The plots show the results for the Schwarzschild, Reissner-Nordström, Kerr and Kerr-Newman black holes for comparison. The critical impact parameter $|b_{sc}|$ decreases as charge Q of the black hole increases.

in agreement with the Kerr case in [3, 34]. In the general situation of finite Q , the solution of r_c becomes

$$r_{sc} = \frac{3M}{2} + \frac{1}{2\sqrt{3}} \sqrt{9M^2 - 8Q^2 + U_c + \frac{P_c}{U_c}} - \frac{s}{2} \sqrt{6M^2 - \frac{16Q^2}{3} - \frac{1}{3} \left(U_c + \frac{P_c}{U_c} \right) + \frac{8\sqrt{3}Ma^2}{\sqrt{9M^2 - 8Q^2 + U_c + \frac{P_c}{U_c}}}, \quad (36)$$

where

$$P_c = (9M^2 - 8Q^2)^2 - 24a^2(3M^2 - 2Q^2),$$

$$U_c = \left\{ (9M^2 - 8Q^2)^3 - 36a^2(9M^2 - 8Q^2)(3M^2 - 2Q^2) + 216M^2a^4 + 24\sqrt{3}a^2 \sqrt{(M^2 - a^2 - Q^2)[Q^2(9M^2 - 8Q^2)^2 - 27M^4a^2]} \right\}^{\frac{1}{3}}. \quad (37)$$

For the Reissner-Nordstrom black holes, $a \rightarrow 0$, we find

$$P_c = U_c^2 = (9M^2 - 8Q^2)^2$$

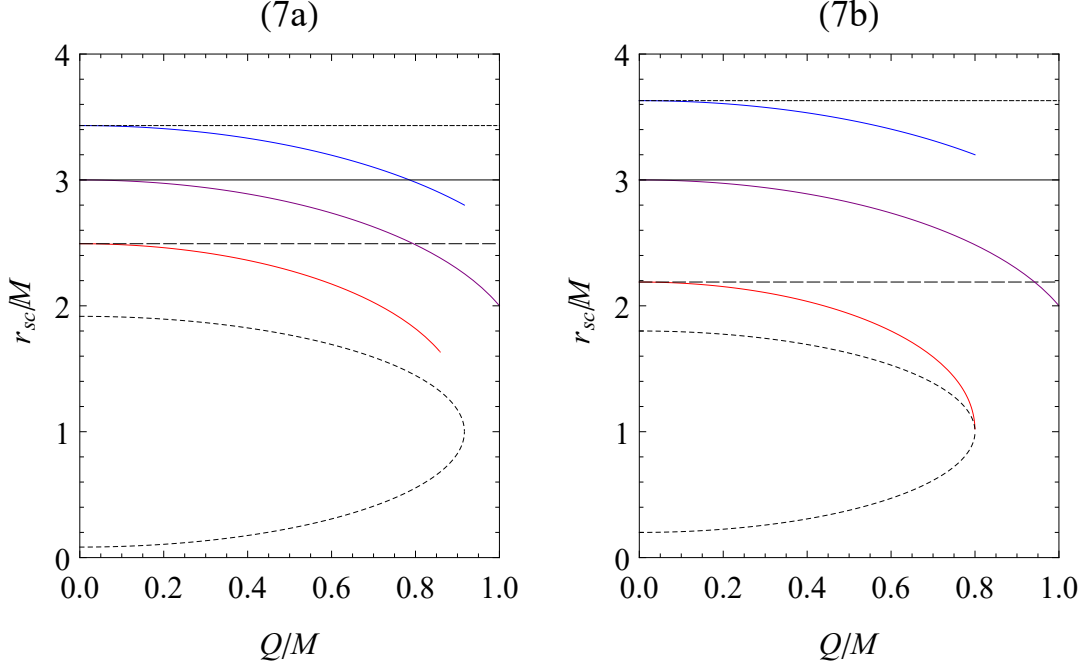


FIG. 7: The critical radius r_{sc}/M as a function of charge Q/M for (a) $a/M = 0.3$, (b) $a/M = 0.6$. The plots of the Schwarzschild, Reissner-Nordström, Kerr and Kerr-Newman black holes are drawn for comparison. Additionally, the Kerr-Newman outer(inner) horizon radii are also shown in red(orange) dashed line for reference. The radius of the innermost circular motion of light rays r_{sc} decreases as charge Q of the black hole increases.

with

$$r_c = \frac{3M}{2} \left(1 + \sqrt{1 - \frac{8Q^2}{9M^2}} \right) \quad (38)$$

as anticipated in [3].

Combining (22) with (18) can derive the following useful relation

$$b_{sc} = a + \frac{r_{sc}^2}{\sqrt{Mr_{sc} - Q^2}}. \quad (39)$$

Thus, substituting the solution of r_{sc} in (36) into the above relation can obtain the result of b_{sc} in terms of the black hole's parameters instead.

Plugging in the value for all parameters, we reproduce the critical impact parameter b_{sc} , and the corresponding radius of the innermost circular motion r_{sc} in Figs.4 and 5, plotted as a function of a for the Kerr black hole [34], and also for the the Kerr-Newman black holes. Due to the fact that the charge of a black hole gives the repulsive effects to the light rays that

prevent them from collapsing into the black hole, it is found that the circular orbits exist for a smaller value of the radius r_{sc} with the smaller impact parameter $|b_{sc}|$ as compared with the Kerr case for the same a . Also, the radius of the innermost circular motion of light rays with the critical impact parameter decreases as charge Q of the black hole increases for both direct and retrograde motions seen in Figs.6 and 7.

IV. THE EXACT EXPRESSION OF EQUATORIAL LIGHT DEFLECTION ANGLE

To obtain the closed-form deflection angle of a light ray due to the Kerr-Newman black hole, we introduce

$$u = 1/r \quad (40)$$

and rewrite (11) and (12), with further combinations, as

$$\left(\frac{du}{d\phi}\right)^2 = \left[\frac{1 - 2Mu + (a^2 + Q^2)u^2}{1 - (2Mu - Q^2u^2)\left(1 - \frac{a}{b_s}\right)} \right]^2 B(u), \quad (41)$$

where the quantity $B(u)$ is a quartic polynomial

$$B(u) = -Q^2 \left(1 - \frac{a}{b_s}\right)^2 u^4 + 2M \left(1 - \frac{a}{b_s}\right)^2 u^3 - \left(1 - \frac{a^2}{b^2}\right) u^2 + \frac{1}{b^2}. \quad (42)$$

The deflection angle $\hat{\alpha}$ as the light ray proceeds in from spatial infinity and back out again is just twice the deflection angle from the turning point $r = r_0$ to infinity. Integrating the equation of motion for ϕ in (41) and subtracting π from it lead to

$$\hat{\alpha} = -\pi + 2 \int_0^{1/r_0} \frac{1 - (2Mu - Q^2u^2)\left(1 - \frac{a}{b_s}\right)}{1 - 2Mu + (a^2 + Q^2)u^2} \frac{du}{\sqrt{B(u)}}. \quad (43)$$

With $B(u)$ that generally has three real positive roots u_2, u_3 , and u_4 and one real negative root u_1 , we can rewrite (42) as

$$B(u) = -Q^2(1 - \omega_s)^2 (u - u_1)(u - u_2)(u - u_3)(u - u_4) \quad (44)$$

with again $\omega_s = a/b_s$. By extending the approach of [34], we parametrize the four roots of $B(u) = 0$ as follows:

$$u_1 = \frac{X - 2M - Y}{4Mr_0}, \quad (45)$$

$$u_2 = \frac{1}{r_0}, \quad (46)$$

$$u_3 = \frac{X - 2M + Y}{4Mr_0}, \quad (47)$$

$$u_4 = \frac{2M}{Q^2} - \frac{X}{2Mr_0}, \quad (48)$$

where we have introduced two functions X and Y , to be determined later. We assume that the functions X and Y in the limit of $Q = 0$ smoothly reduce to the corresponding functions in a Kerr black hole in [34]. If so, by taking the $Q = 0$ limit, the function $B(u)$ in a Kerr black hole in [34] can be recovered from (44), where the root u_4 is removed. Comparing the coefficients of different powers of u in $B(u)$ to those in the original polynomial in (42), we obtain the equations to determine the functions X and Y as follows:

$$Q^2 [Y^2 - (X - 2M)(X + 6M) + 4X^2] = 16M^2r_0 \left(X - r_0 \frac{1 + \omega_s}{1 - \omega_s} \right), \quad (49)$$

$$Y^2 - (X - 2M)^2 = \frac{8M(X - 2M)(Q^2X - 4M^2r_0)}{Q^2(X - 2M) - 4M^2r_0}, \quad (50)$$

$$[Y^2 - (X - 2M)^2] \left(\frac{1}{8Mr_0^3} - \frac{Q^2X}{32M^3r_0^4} \right) = \frac{1}{b^2(1 - \omega_s)^2}. \quad (51)$$

Notice that these equations are given in terms of the black hole's parameters as well as the distance of closest approach r_0 of a light ray with the impact parameter b . Substituting (49) into (51) reproduces (18), which shows that $1/r_0$ is one of the roots. The combination of (49) and (50), with further rearrangement, gives a cubic equation of X ,

$$\begin{aligned} \frac{Q^2}{2M}X^3 - (Q^2 + 4Mr_0)X^2 + \left(4M^2r_0 + 2MQ^2 + \frac{8M^3r_0^2}{Q^2} + \frac{2Mr_0^2(1 + \omega_s)}{(1 - \omega_s)} \right) X \\ = 4M^2Q^2 + \frac{4M^2r_0^2(1 + \omega_s)}{1 - \omega_s} + \frac{8M^3r_0^3(1 + \omega_s)}{Q^2(1 - \omega_s)}. \end{aligned} \quad (52)$$

We can solve directly the cubic equation (52), and one of three roots is

$$\begin{aligned} X(M, Q, r_0, \omega_s) = \frac{2M(Q^2 + 4Mr_0)}{3Q^2} \\ + \frac{8M^2r_0}{3Q^2} \sqrt{1 + \frac{Q^2}{2M^2r_0} \left(M - \frac{3r_0(1 + \omega_s)}{2(1 - \omega_s)} - \frac{Q^2}{r_0} \right) \cos \left(\frac{\Theta_X}{3} + \frac{2\pi}{3} \right)}, \end{aligned} \quad (53)$$

where

$$\Theta_X = \arccos \left[\frac{-8M^3r_0^3 - 3MQ^2r_0^2 \left(2M - \frac{3r_0(1+\omega_s)}{(1-\omega_s)} \right) - 3Q^4r_0 \left(5M - \frac{3r_0(1+\omega_s)}{(1-\omega_s)} \right) + 10Q^6}{\left[4M^2r_0^2 + Q^2r_0 \left(2M - \frac{3r_0(1+\omega_s)}{(1-\omega_s)} \right) - 2Q^4 \right]^{\frac{3}{2}}} \right]. \quad (54)$$

The limit of $Q = 0$ leads to $\Theta_X = \pi$. In this case Eq. (53) can be simplified enormously as

$$X(M, Q = 0, r_0, \omega_s) = r_0 \frac{(1 + \frac{a}{b_s})}{(1 - \frac{a}{b_s})}, \quad (55)$$

which agrees with the result in [34]. Next, using the solutions of r_0 in (19) and X in (53), from (50) one can find the function Y in terms of (a, Q, b, s, r_0) . Thus, we have successfully generalized the expressions of the Kerr black hole case in [34] to those of a Kerr-Newman black hole. They become very crucial, as seen later, to obtain an expression of the deflection angle of light rays in terms of the elliptic functions.

In the case of the Reissner-Nordstrom black holes ($a \rightarrow 0$), the expression in the bracket of the deflection angle (41) reduces to 1. Moreover, as discussed in [3], the equation $B(u) = 0$ has four roots as in the Kerr-Newman case, in particular evaluating r_0 at r_c in (38) gives $X = 2M(\frac{2Mr_c}{Q^2} - 1)$ in (53), which is the solution of (52) in the limit of $a \rightarrow 0$. As such, the root of u in (48) is then $u_4 = \frac{1}{r_c}$, and together with u_2 becomes double roots at $\frac{1}{r_c}$. Here we have found four roots in a general r_0 for nonzero Q and a , consistent with the findings in the literature by taking an appropriate limit for Kerr black holes ($a \neq 0, Q = 0$) or a Reissner-Nordstrom black hole ($Q \neq 0, a = 0$).

To proceed, we first write the function in the bracket of (41) as

$$\begin{aligned} & \frac{1 - 2Mu(1 - \omega_s)}{1 - 2Mu + (a^2 + Q^2)u^2} + \frac{Q^2u^2(1 - \omega_s)}{1 - 2Mu + (a^2 + Q^2)u^2} \\ &= \frac{C_+}{u_+ - u} + \frac{C_-}{u_- - u} + \frac{C_{Q+}u}{u_+ - u} + \frac{C_{Q-}u}{u_- - u}, \end{aligned} \quad (56)$$

where

$$u_{\pm} = \frac{M \pm \sqrt{M^2 - (a^2 + Q^2)}}{a^2 + Q^2}. \quad (57)$$

Solving for C_+ , C_- , C_{Q+} and C_{Q-} , we obtain

$$\begin{aligned}
C_+ &= \frac{2M(1 - \omega_s) \left(M + \sqrt{M^2 - (a^2 + Q^2)} \right) - (a^2 + Q^2)}{2(a^2 + Q^2)\sqrt{M^2 - (a^2 + Q^2)}}, \\
C_- &= \frac{(a^2 + Q^2) - 2M(1 - \omega_s) \left(M - \sqrt{M^2 - (a^2 + Q^2)} \right)}{2(a^2 + Q^2)\sqrt{M^2 - (a^2 + Q^2)}}, \\
C_{Q+} &= \frac{-Q^2(1 - \omega_s) \left(M + \sqrt{M^2 - (a^2 + Q^2)} \right)}{2(a^2 + Q^2)\sqrt{M^2 - (a^2 + Q^2)}}, \\
C_{Q-} &= \frac{Q^2(1 - \omega_s) \left(M - \sqrt{M^2 - (a^2 + Q^2)} \right)}{2(a^2 + Q^2)\sqrt{M^2 - (a^2 + Q^2)}}.
\end{aligned} \tag{58}$$

The integral form of deflection angle in (43) is then

$$\hat{\alpha} = -\pi + 2 \int_0^{1/r_0} \left(\frac{C_+}{u_+ - u} + \frac{C_-}{u_- - u} + \frac{C_{Q+} u}{u_+ - u} + \frac{C_{Q-} u}{u_- - u} \right) \frac{1}{\sqrt{B(u)}} du \tag{59}$$

where $B(u)$ is written as a product of the roots in (44). The exact expression of bending angle consequently is given in terms of elliptical integrals as [44]

$$\begin{aligned}
\hat{\alpha} &= -\pi + \frac{4}{(1 - \omega_s)\sqrt{Q^2(u_4 - u_2)(u_3 - u_1)}} \\
&\cdot \left\{ \frac{C_+ + C_{Q+}u_1}{u_+ - u_1} [\Pi(n_+, k) - \Pi(n_+, \psi_0, k)] + \frac{C_- + C_{Q-}u_1}{u_- - u_1} [\Pi(n_-, k) - \Pi(n_-, \psi_0, k)] \right. \\
&\quad - \frac{C_+ + C_{Q+}u_4}{u_+ - u_4} [\Pi(n_+, k) - \Pi(n_+, \psi_0, k) - K(k) + F(\psi_0, k)] \\
&\quad \left. - \frac{C_- + C_{Q-}u_4}{u_- - u_4} [\Pi(n_-, k) - \Pi(n_-, \psi_0, k) - K(k) + F(\psi_0, k)] \right\}.
\end{aligned} \tag{60}$$

In (60),

$$\begin{aligned}
n_{\pm} &= \frac{u_2 - u_1}{u_{\pm} - u_1} \left[1 + \frac{2MQ^2(1 - r_0u_{\pm})}{4M^2r_0 - Q^2(X + 2M)} \right], \\
k^2 &= \frac{(Y + 6M - X) [8M^2r_0 - Q^2(Y - 2M + 3X)]}{4Y [4M^2r_0 - Q^2(X + 2M)]}, \\
\psi_0 &= \arcsin \sqrt{\frac{(Y + 2M - X) [4M^2r_0 - Q^2(X + 2M)]}{(Y + 6M - X)(4M^2r_0 - Q^2X)}},
\end{aligned} \tag{61}$$

and $\Pi(n_+, k)$ and $\Pi(n_+, \psi_0, k)$ are, respectively, the complete and the incomplete elliptic integrals of the third kind. Additionally, $K(k)$, the complete elliptic integral of the first kind, and $F(\psi_0, k)$, the incomplete elliptic integral of the first kind, are also involved. In

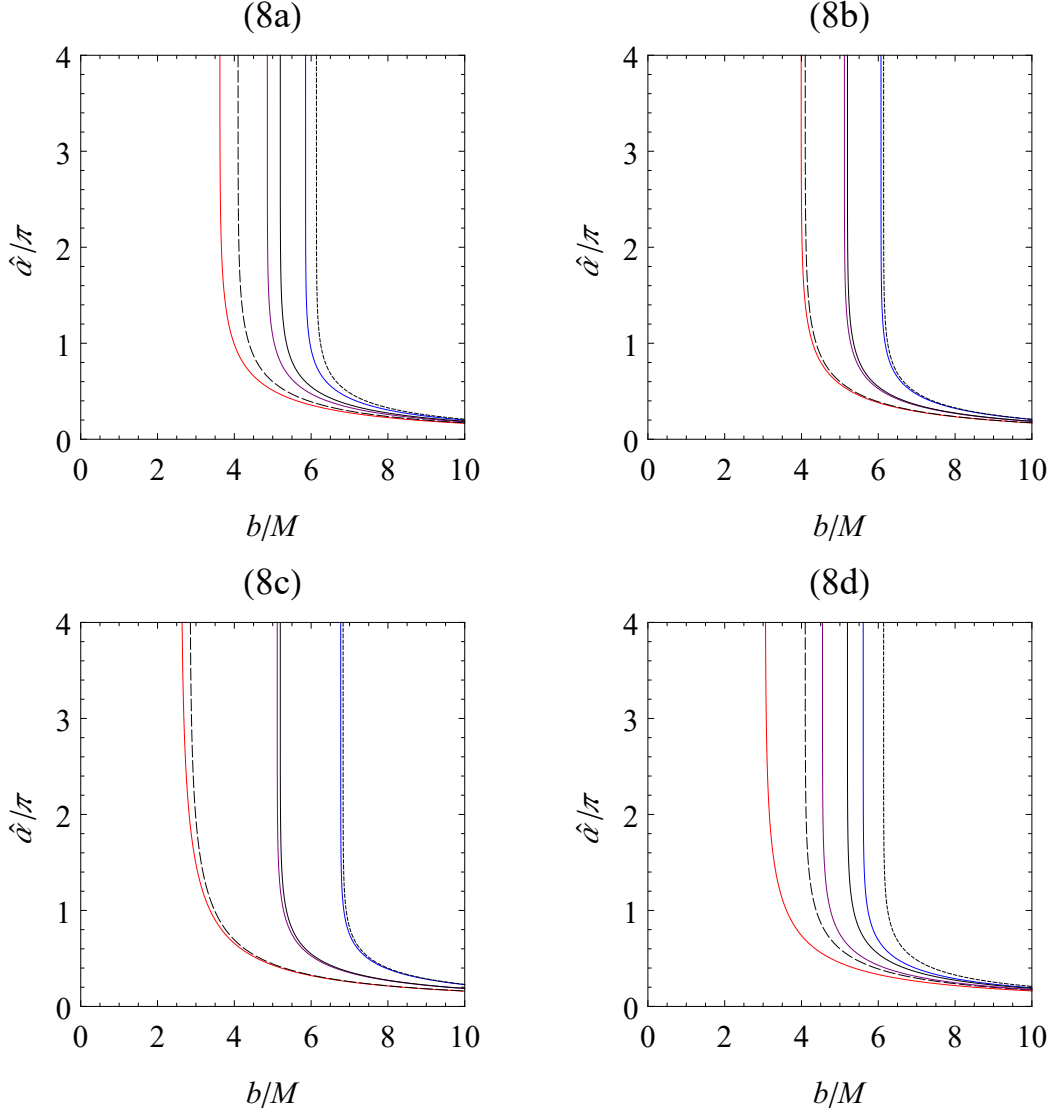


FIG. 8: Deflection angle as a function of impact parameter b/M for four sets of parameters. (a) $a/M = 0.5$, $Q/M = 0.6$; (b) $a/M = 0.5$, $Q/M = 0.3$; (c) $a/M = 0.9$, $Q/M = 0.3$; (d) $a/M = 0.5$, $Q/M = 0.8$. The plots show the results for the Schwarzschild, Reissner-Nordstrom, Kerr and Kerr-Newman black holes for comparison. The suppression of the bending angle for light rays due to the charged black hole as compared with the corresponding black hole with $Q = 0$ is found for the same impact parameter b .

particular, the condition $0 \leq k^2 \leq 1$ has been checked numerically. This is one of the main results of the work.

It is quite straightforward to find that in the $Q = 0$ limit, the whole expression of (60) reduces to that of the Kerr black hole in [34]. Additionally, the deflection angle (60) in

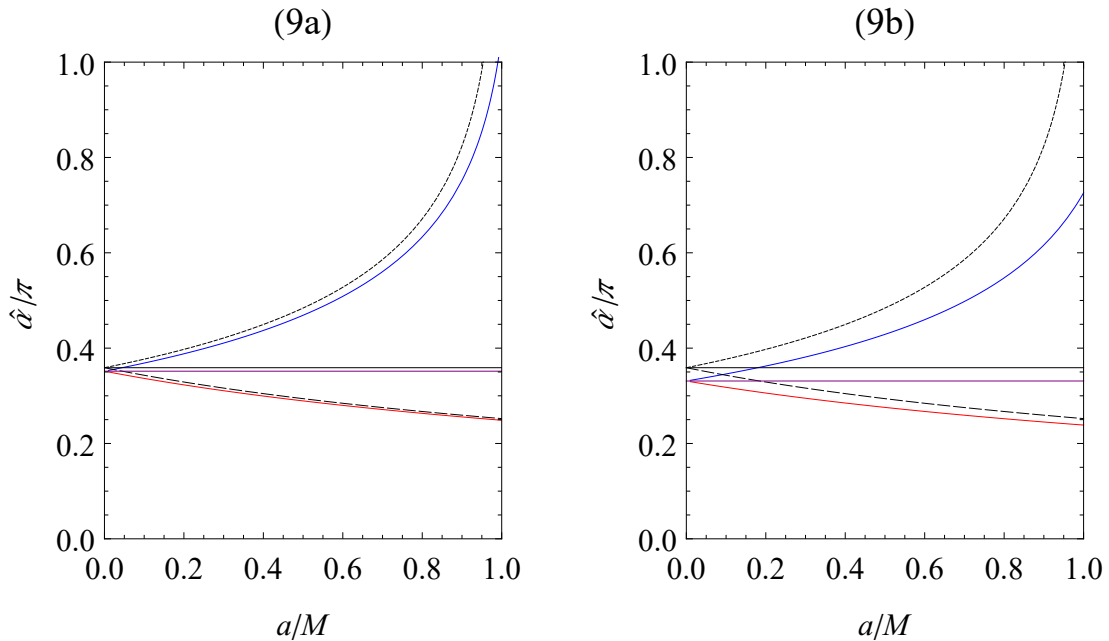


FIG. 9: Deflection angle as a function of spin parameter a/M for (a) $Q/M = 0.3$, and $b = 7M$; (b) $Q/M = 0.6$, and $b = 7M$. The plots show the results for the Schwarzschild, Reissner-Nordstrom, Kerr and Kerr-Newman black holes for comparison. The nonzero charge of the black hole decreases the deflection angle also due to the additional repulsive effects on the light rays for the fixed spin of black hole a and the given impact parameter of the light ray b .

the limit of $a \rightarrow 0$ gives the closed-form expression of the bending angle of light rays due to the Reissner-Nordstrom black holes. Numerical studies in Fig.8 reproduce the deflection angle of light rays due to the Schwarzschild ($Q \rightarrow 0, a \rightarrow 0$) and Kerr black holes ($Q \rightarrow 0$) as a function of the impact parameter b in [34]. However, in the Kerr-Newman case, one of the remarkable results is the suppression of the bending angle compared with the Kerr case due to the repulsive effects from the black hole's charge to the light rays for a fixed impact parameter in both direct and retrograde motions. These effects can be realized in Fig.9, and also in particular in Fig.10 where the deflection angle $\hat{\alpha}$ decreases as the charge Q of the black hole increases. This will result in the modification of the apparent shadows from the Kerr case as it has been seen in [40]. The shadow of the black hole is perceived by an observer at spatial infinity at different polar positions. Based upon our results, it is anticipated that the larger charge Q with a fixed black hole spin and the polar positions

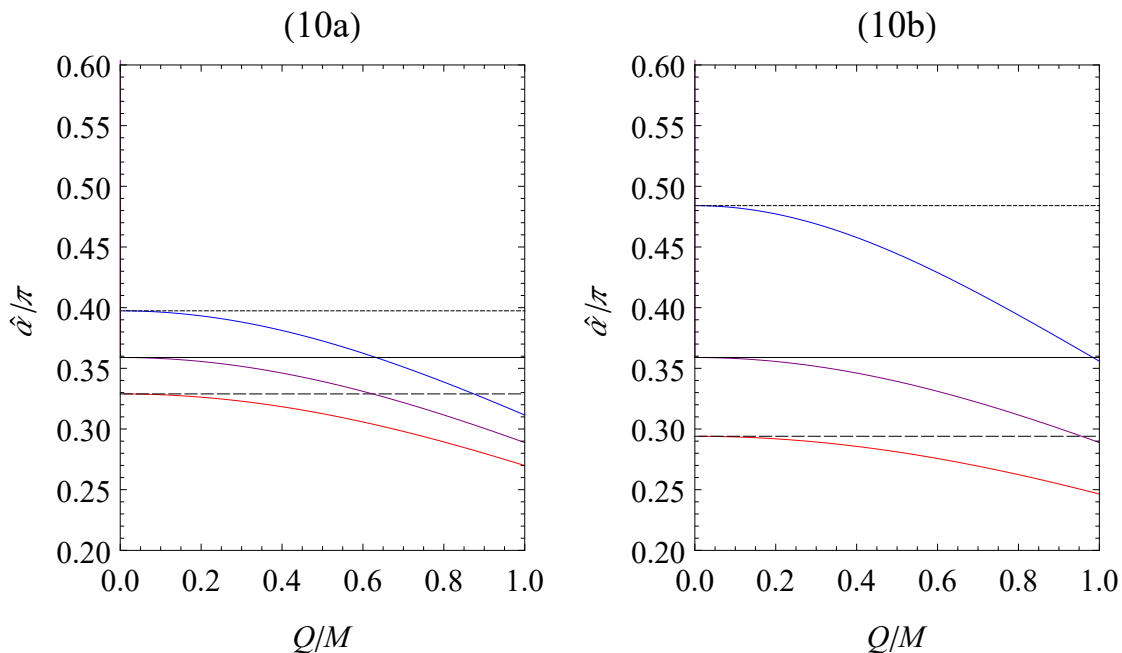


FIG. 10: Deflection angle as a function of charge Q/M for (a) $a/M = 0.2$, and $b = 7M$; (b) $a/M = 0.5$, and $b = 7M$. The plots show the results for the Schwarzschild, Reissner-Nordstrom, Kerr and Kerr-Newman black holes for comparison. The deflection angle decreases as the charge Q of the black hole increases for a given impact parameter b .

of the observers leads to the smaller boundary of the shadow of the Kerr-Newman black holes that will be further explored in our future work. Our approach gives a closed-form expression of the deflection angle of the light rays due to the Kerr-Newman black hole that certainly generalizes the Kerr case in [34], and also explores the effect from the charge of the black hole to the light bending with an appropriate “effective potential” defined from the radial motion of a light ray.

V. SUMMARY AND OUTLOOK

In summary, the dynamics of light rays traveling around a Kerr-Newman black hole is studied with emphasis on how the charge of black holes influences their trajectories. We first examine the innermost circular orbits on the equatorial plane. It is found that the presence of the charge of the black hole results in the “effective potential” which is defined from the equation of motion of light rays along the radial direction, with stronger repulsive effects as

compared with the Kerr black hole. As a result, the radius of the innermost circular motion of light rays decreases as charge Q of the black hole increases for both direct and retrograde motions, which certainly gives a direct consequence on constructing the apparent shape of a charged rotating black hole. We then derive the closed-form expression of the deflection angle in terms of elliptic integrals by generalizing the work of [34]. The nonzero charge of the black hole decreases the deflection angle also due to the additional repulsive effects on the light rays given by the “effective potential” of the photon radial motion. In the next step, we will study this analytical solution in the form of series expansion in the strong and weak deflection regimes, and compare with the works of [36, 45] for the Kerr case. The accurate and efficient approximation schemes can be an attractive alternative to compute the involved elliptical integrals in black hole simulations.

Acknowledgments

This work was supported in part by the Ministry of Science and Technology, under Grant No. 108-2112-M-259-002.

-
- [1] C. W. Misner, K. S. Thorne, and J. A. Wheeler, *Gravitation* (W. H. Freeman and Company, San Francisco, 1973).
 - [2] J. B. Hartle, *Gravity: An Introduction to Einstein’s General Relativity* (Addison-Wesley, Reading, MA, 2003).
 - [3] S. Chandrasekhar, *The Mathematical Theory of Black Holes* International Series of Monographs on Physics. Vol. 69 (Clarendon Press/Oxford University Press, Oxford, 1993).
 - [4] K. Akiyama *et al.* (Event Horizon Telescope Collaboration), *Astrophys. J.* **875**, L1 (2019).
 - [5] K. Akiyama *et al.* (Event Horizon Telescope Collaboration), *Astrophys. J.* **875**, L5 (2019).
 - [6] K. Akiyama *et al.* (Event Horizon Telescope Collaboration), *Astrophys. J.* **875**, L6 (2019).
 - [7] C. Darwin, *Proc. R. Soc. A* **249**, 180 (1959).
 - [8] J.-P. Luminet, *Astron. Astrophys.* **75**, 228 (1979).
 - [9] H.C. Ohanian, *Am. J. Phys.* **55**, 428 (1987).
 - [10] R.J. Nemiro, *Am. J. Phys.* **61**, 619 (1993).

- [11] V. Bozza, S. Capozziello, G. Iovane, and G. Scarpetta, *Gen. Relativ. Gravit.* **33**, 1535 (2001).
- [12] E.F. Eiroa, G.E. Romero, and D. Torres, *Phys. Rev. D* **66**, 024010 (2002).
- [13] M. Sereno, *Phys. Rev. D* **69**, 023002 (2004).
- [14] C. R. Keeton and A. O. Petters, *Phys. Rev. D* **72**, 104006 (2005).
- [15] A. Bhadra, *Phys. Rev. D* **67**, 103009 (2003).
- [16] V. Bozza, *Phys. Rev. D* **66**, 103001 (2002).
- [17] K.S. Virbhadra and G.F.R. Ellis, *Phys. Rev. D* **62**, 084003 (2000).
- [18] K.S. Virbhadra and C.R. Keeton, *Phys. Rev. D* **77**, 124014 (2008).
- [19] K.S. Virbhadra, *Phys. Rev. D* **79**, 083004 (2009).
- [20] S. Vazquez and E. Esteban, *Nuovo Cimento Soc. Ital. Fi.* **119B**, 489 (2004).
- [21] V. Bozza, F. De Luca and G. Scarpetta, *Phys. Rev. D* **74**, 063001 (2006).
- [22] V. Bozza and G. Scarpetta, *Phys. Rev. D* **76**, 083008 (2007).
- [23] V. Bozza, *Phys. Rev. D* **78**, 063014 (2008).
- [24] G.V. Kraniotis, *Classical Quantum Gravity* **28**, 085021 (2011).
- [25] A.B. Aazami, C.R. Keeton, and A.O. Petters, *J. Math. Phys. (N.Y.)* **52**, 092502 (2011).
- [26] A.B. Aazami, C.R. Keeton, and A.O. Petters, *J. Math. Phys. (N.Y.)* **52**, 102501 (2011).
- [27] R. Takahashi, *Astrophys. J.* **611**, 996 (2004).
- [28] A.F. Zakharov, A.A. Nucita, F. De Paolis, and G. Ingrosso, *New Astron.* **10**, 479 (2005).
- [29] A.F. Zakharov, F. De Paolis, G. Ingrosso, and A.A. Nucita, *Astron. Astrophys.* **442**, 795 (2005).
- [30] K. Hioki and U. Miyamoto, *Phys. Rev. D* **78**, 044007 (2008).
- [31] C. Bambi and K. Freese, *Phys. Rev. D* **79**, 043002 (2009).
- [32] K. Hioki and K.I. Maeda, *Phys. Rev. D* **80**, 024042 (2009).
- [33] L. Amarilla, E.F. Eiroa and G. Giribet, *Phys. Rev. D* **81**, 124045 (2010).
- [34] S. V. Iyer and E. C. Hansen, *Phys. Rev. D* **80**, 124023 (2009).
- [35] S. V. Iyer and A. O. Petters, *Gen. Relativ. Gravit.* **39**, 1563 (2007).
- [36] N. S Barlow, S. J Weinstein and J. A. Faber, *Classical Quantum Gravity* **34**, 135017 (2017).
- [37] R. J. Beachley, M. Mistysyn, J. A. Faber, S. J. Weinstein, and N. S. Barlow, *Classical Quantum Gravity* **35**, 205009 (2018); **35**, 229501(E) (2018).
- [38] T. Damour, R. Hanni, R. Ruffini, and J. Wilson, *Phys. Rev. D* **17**, 1518 (1978).
- [39] N. Dadhich and P. P. Kale, *J. Math. Phys. (N.Y.)* **18**, 1727 (1977).

- [40] A. de Vries, *Classical Quantum Gravity* **17**, 123 (2000).
- [41] Z. Stucklik and S. Hledik, *Classical Quantum Gravity* **17**, 4541 (2000).
- [42] S. Chakraborty and A. K. Sen, *Classical Quantum Gravity* **32** 115011 (2015).
- [43] C.-Y. Liu, D.-S. Lee, and C.-Y. Lin, *Classical Quantum Gravity*, **34**, 235008 (2017).
- [44] I. S. Gradshteyn and I. M. Ryzhik, *Tables of Integrals, Series, and Products*, 7th ed. (Academic Press, New York, 2007).
- [45] S. V. Iyer and E. C. Hansen, arXiv:0908.0085.